Lagrangian single-column modeling of Arctic airmass transformation during HALO-($\mathscr{AC}$)^3

Michail Karalis[1], Gunilla Svensson[1,2], Manfred Wendisch[3], Michael Tjernström[1]

[1]Stockholm University, Department of Meteorology and Bolin Centre for Climate Research, Stockholm, Sweden

[2]KTH Royal Institute of Technology, Department of Engineering Mechanics, FLOW, Stockholm, Sweden

[3]Leipzig Institute for Meteorology (LIM), Leipzig University, Leipzig, Germany

July 23, 2025

We would like to thank the ACP editor and all anonymous referees for their insightful reviews of the manuscript. Below you may find our responses (regular font text) to each of the referee's remarks (gray text) along with the respective changes made in the manuscript (**"bold text"**)

Referee #1

Summary

In this study, Karalis and coauthors study the transformation of an air mass entering the Atlantic sector of the Arctic during March 2022. They use observations from the HALO-(AC)3 field campaign along with a single-column model to dissect the physical processes occurring within the air mass and validate the model simulations. They find that different physical processes influence the air mass cooling along its path, with near-surface radiative and turbulent cooling dominating over the ocean, and cloud processes and adiabatic cooling becoming more important as the air mass progresses into the marginal ice zone and sea ice areas. They also find that the single-column model generally simulates the air mass transformation realistically, but struggles to reproduce the stable boundary layer and is highly dependent on the vertical motion prescribed by the ERA5 reanalysis data used to force the model.

This study provides a unique perspective on Arctic air mass transformation, a process that is still not fully understood but is critically important to understanding the causes of Arctic-amplified warming. The paper is generally well-written and scientifically robust. I have a number of minor comments and technical corrections listed below. Once these comments are addressed, in my evaluation this will be a valuable addition to the literature on Arctic air mass transformation.

We thank the reviewer for their positive review and insightful comments which helped improve the state of the manuscript considerably.

Minor comments

- General comment: Is this air mass considered to be "fully transformed" at the end of the 12–14 March 2022 study period, or did it continue cooling after the HALO-(AC)3 sampling ended on 14 March? At the end of the study period, was the air temperature characteristic of a cold Arctic air mass, or was its thermal state more characteristic of an air mass still in transition from mid-latitude to Arctic conditions? If it continued cooling, do the authors expect that the dominant cooling processes at the end of the study period continued to be most important for air mass cooling as the air continued to reside in the Arctic? From Fig. 4 it appears the air mass was still cooling, albeit at possibly a cooler rate, at the end of the study period. I understand that further simulations outside the study period are likely outside of the scope of this study, but it would be useful to provide some discussion about these aspects for context.

A: Thank you for raising this point. The airmass is, indeed, not fully transformed by the end of the simulation period. With an integrated water vapor (IWV) content of 8 kg m^{-2}, it is still anomalously moist (and subsequently warm) compared to the 1979-2019 climatological median of approximately 2 kg m^{-2} (Rinke et al., 2021). The future of the remaining heat and moisture will be determined by:

1. Its residence time in the Arctic. Airmasses take, on average, 5 days to cross the Arctic (Woods and Caballero, 2016) . Depending on the dominant mechanisms in each case, this may not be enough time for an airmass to be entirely transformed by the time it exits the region. In this specific case, the second warm-air intrusion that took place the next day (March 15) will likely mix with the left-over moisture from the previous episode and cease the transformation process prematurely.

2. The large-scale dynamic conditions. The updraft that dominated the second half of the transformation forced a moisture loss of around 5 kg m^{-2}. If that were to be sustained for longer, IWV could drop to typical Arctic airmass values in the next 24 hours. In milder subsidence conditions, temperature changes would be driven mostly by radiative cooling (Fig AR1.1). The emitted longwave radiation, however, would grow weaker as the temperature drops and the liquid clouds dissipate, requiring more time for the transformation to reach completion.

We added the following lines in Sect. 3.3.6

L498-509: "It should be noted that, at the end of the the simulation period, the airmass has an IWV_{5km} of 8 kg m^{-2}, which makes it still anomalously moist (and subsequently warm) compared to the 1979-2019 climatological median of approximately 2 kg m^{-2} (Rinke et al., 2021). The airmass transformation is, therefore, not complete and could continue for several days as is typical for WAIs in the Atlantic sector (Woods and Caballero, 2016). In this specific case, the second warm-air intrusion that is set up to take place the next day (March 15) will likely mix with the left-over moisture from the previous episode and cease the transformation process prematurely. But large-scale dynamics are important for the future of the remaining heat and moisture even before the merge. The large-scale updraft that dominated the transformation over sea-ice resulted in a temperature decrease of 6 ºC, triple in magnitude

that that exerted by radiation and turbulent mixing combined (Fig. C1). If the airmass continued to be lifted and, thus, losing heat and moisture at the same rate, IWV could drop to typical Arctic airmass values in the next 24 hours. In milder subsidence conditions, temperature changes would be driven mostly by radiative cooling (Fig. C1). The emitted longwave radiation, however, would grow weaker as the temperature drops and the liquid clouds dissipate, requiring more time for the transformation to reach completion. ”

- General comment: The authors provide qualitative descriptions of which physical processes were most important for air mass cooling at different stages of its life cycle. Is it possible to integrate these contributions over time to provide a comparison of which processes contributed the most to cooling throughout the entire study period?

A: Thank you for this suggestion. We computed the contributions of the participating processes by integrating the temperature changes in time and height (up to 5 km). This shows adiabatic cooling as the biggest contributor to the airmass transformation, followed by radiation (Fig. AR1.1). The only consistent heat source for the airmass is latent heat release from cloud condensation which then drives the moisture depletion. We include the figure in Appendix C (Fig. C1)

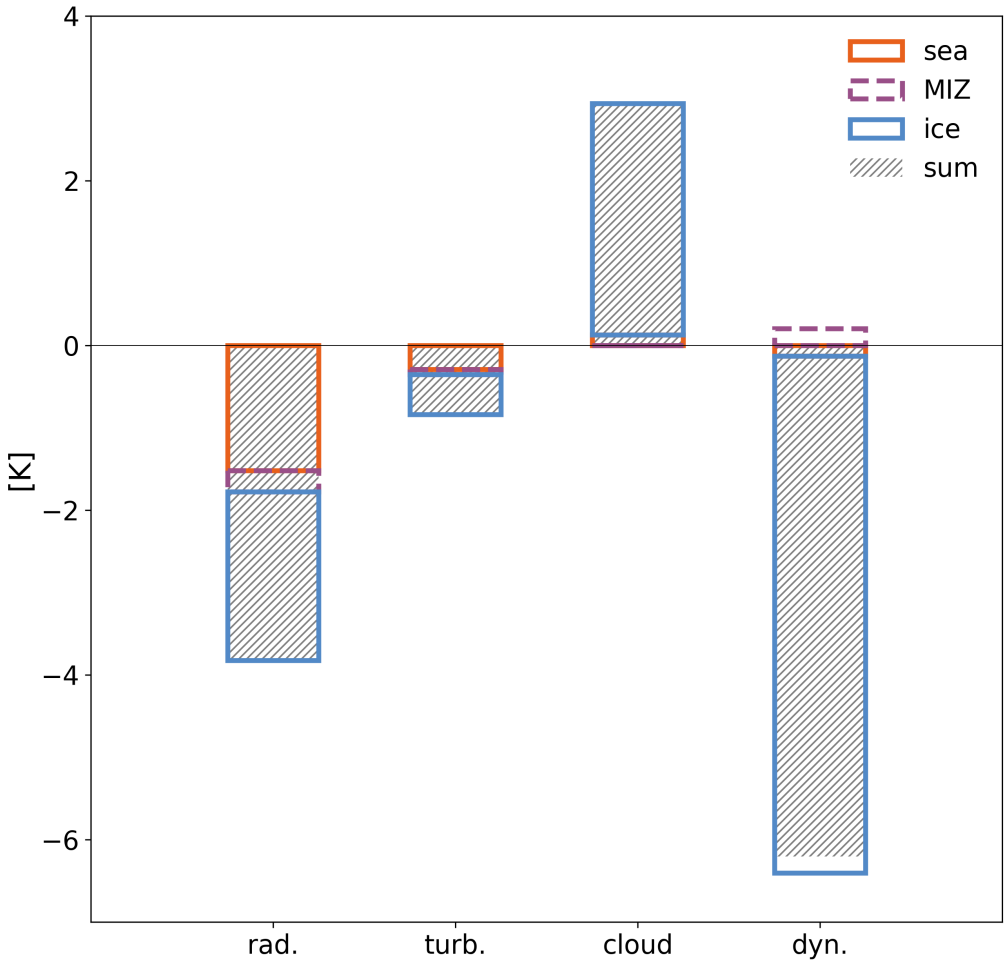

Figure AR1.1: Integrated temperature changes contributed by radiation, turbulence, cloud processes and adiabatic cooling. Different colors are used to show the changes per transformation leg (ocean, MIZ, ice) and hatches to show the sum over the entire transformation.

- L6: The meaning of "undistorted" air column isn't quite clear here and doesn't become apparent until later in the paper (e.g. L99–101, L112–118, L180–191). I suggest using the word "cohesive" in the abstract (as in L182) to be more clear.

A: Thank you. We changed it to the proposed phrasing (**L6**)

- L150–152: What type of adjustment is needed for the model to be able to produce realistic skin temperature values?

A: The surface energy budget from the incoming warm and moist airmass leads to a quick increase in the skin temperature. Skin temperature is the variable through which the air-column is coupled to the surface as it participates in the calculation of surface energy fluxes. Thus, the fast adjustment of the surface to the overlying column becomes problematic when trying to study the Lagrangian airmass transformation, big part of which is the response of the airmass to the constantly varying surface conditions.

We kept the skin temperature from increasing by initializing the sea-ice with larger internal energy values or, in simpler terms, colder sea-ice temperatures than the reanalysis in the representative region. This causes the downward conductive heat flux to counterbalance the incoming energy and maintains a colder skin temperature. For reference, for the 25 h long "ice" leg, the simulated mean sea-ice temperature goes from approximately -32 ºC to -28 ºC, the sea-ice surface temperature increases from -33 ºC to -13 ºC while the snow skin temperature adjusts at approximately -8 ºC and remains constant for the entire leg (Fig. AR1.2). This procedure gives a more advanced coupling to the sea ice than the limited options through prescribing surface values. Fig. AR1.2 is now offered in Appendix B.

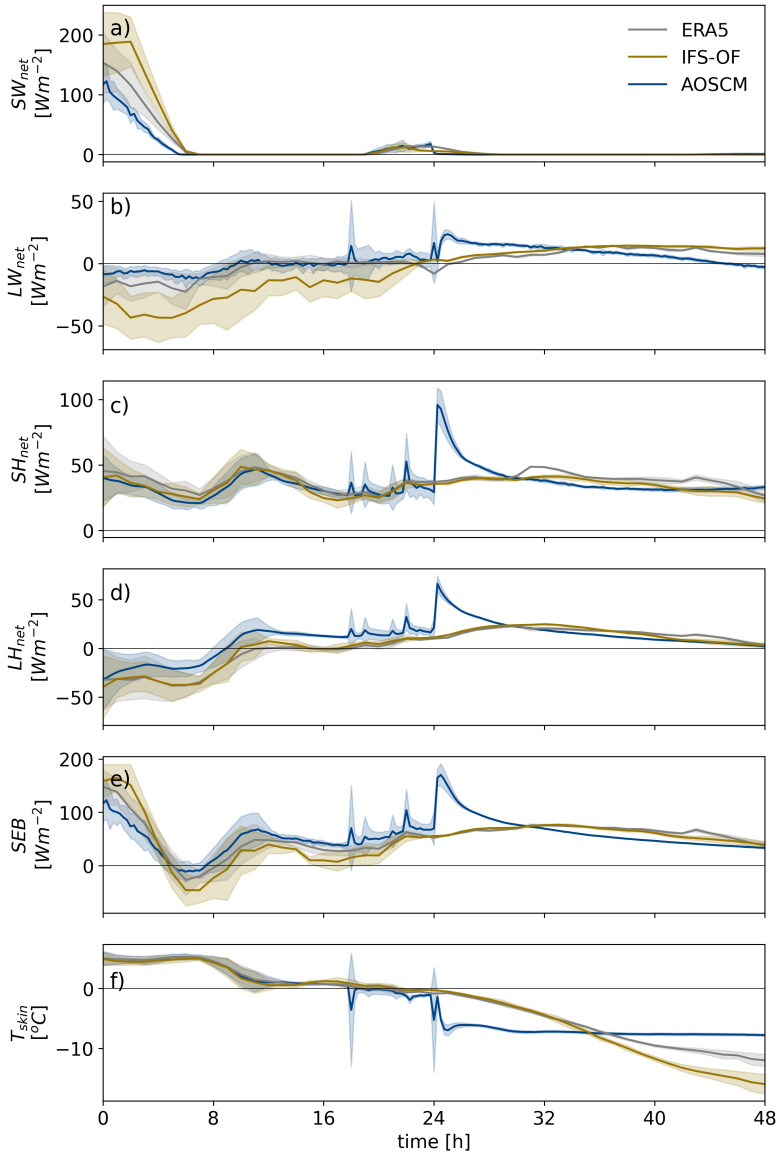

Figure AR1.2: Time-series of the surface a) shortwave radiative, b) longwave radiative, c) sensible heat, d) latent heat fluxes, e) the surface energy budget and f) the skin temperature along the trajectories. The AOSCM, ERA5 and IFS-OF are drawn with blue, grey and sand respectively.

This is not an optimal fix but, it helps realistically simulate the airmass Lagrangian evolution by

ensuring fluxes of comparable magnitude to ERA5 and the operational forecast IFS-OF. Additionally, this treatment is specific to this application and this version of the AOSCM where LIM3 is used as a sea-ice model. In future studies, working with newer versions of AOSCM in which LIM3 has been replaced with SI3, we can achieve similar results by breaking up the airmass trajectory to smaller legs and re-initializing the sea-ice properties more frequently. We have added the following sentence in the manuscript.

L174-177: " ~~ERA5 is also used for the initialization of sea-ice temperature, although an adjustment is necessary for the model to be able to produce realistic skin temperature values, comparable to the respective mean ERA5 values for each leg.~~ **We initialize the sea ice at lower temperatures than indicated by reanalysis. This causes the downward conductive heat flux to counterbalance the incoming energy, maintaining a colder skin temperature, comparable to the respective mean ERA5 values for each leg (Fig. B1f, Table 1). As a result, the surface fluxes are closer to ERA5 (Fig. B1a-e). "**

- L145–154: I'm not entirely clear on the mixture of data sources here. So ERA5 is used for SIC, then CMEMS is used to quantify snow on top of sea ice and sea ice thickness? So both the snow on sea ice and the sea ice thickness are taken into account by the AOSCM? This is also unclear in L364–366.

A: The AOSCM requires sea-ice and snow thickness information to be given as input. However, this information is not available in ERA5. Instead, we take characteristic values for the MIZ and sea-ice legs respectively from CMEMS. We used ERA5 to initialize sea-ice concentration but values are similar in both reanalyses.

We realize that merely describing the various datasets does not necessarily reflect the differences in the sea-ice properties between the different simulation legs. We, therefore, introduce Table 1. in Sect. 2.4 of the manuscript in which we explicitly present the values used for the sea-ice properties of each leg.

"

Table 1. Representative values for sea-ice and snow properties used in the coupled simulations.

	MIZ	ice
Sea-ice concentration	60 %	99 %
Ice thickness	0.90 m	2.1 m
Snow thickness	0.13 m	0.31 m
Skin temperature	~ -1.5 °C	~ -8 °C

"

- Fig. 2 and Fig. 3: Are these maps showing instantaneous snapshots of IVT, IWV, LWP, etc.? Or are these quantities integrated over time? Is the (Eulerian) ERA5 regular grid field of these values

plotted, or are the values interpolated to the Lagrangian trajectories? I assume the cloud fields (LWP, IWP) and SEB values (SHF, LHF, etc.) are taken from ERA5, is this correct?

A: All variables shown in Fig. 2c and Fig. 3 are taken from ERA5. These plots show the Lagrangian evolution of each variable along and around the airmass trajectories rather than a snapshot of the fields at any specific moment. It may be helpful to think of the trajectories in these plots as a time axis. At each timestep the airmass around the trajectories is detected and visualized according to the airmass tracking method described in Sect. 2.3. These Lagrangian maps show the width of the airmass with respect to the width of the trajectory ensemble, with the latter representing the size of the air-column our study focuses on, and reveal the amount of variability that exists within the airmass. We have edited **Fig. 2c's caption** to help the reader interpret the figure more easily.

"c) ~~temporal evolution and spatial variability of integrated water vapor transport (IVT). The trajectory ensemble is shown with black lines. Hatches mark the correlation range (see Sect. 2.3) around the airmass at each timestep.~~ **Map of the temporal evolution and spatial variability of integrated water vapor transport (IVT). The trajectory ensemble, drawn with black lines, serves the purpose of a time axis. IVT changes in the direction parallel to the trajectories show the temporal evolution of the airmass. IVT changes in the direction perpendicular to the trajectories show the spatial variability of the airmass at the respective timestep (12/03/2022, 12 UTC at the southernmost point to 14/03/2022, 12 UTC at the northernmost). Hatches mark the correlation range showing areas around the trajectories of similar vertical structure at each timestep (see Sect. 2.3). "**

- L206–208: This is an interesting hypothesis about the quality controls in the assimilation scheme filtering the profiles out – is there any way to check this?

A: Ehrlich et al., (2025) reported that none of the dropsonde profiles collected during this WAI event were submitted to the Global Telecommunication System (GTS). Therefore, no observations from flights RF02, RF03 and RF04 were assimilated in ERA5 which makes their in-between mismatch a lot more reasonable. We update our statement about dropsonde assimilation and relevant discussion accordingly:

L233-235: "~~The profiles located on the eastern boundary of the airmass show a consistent mismatch with ERA5 data, in most cases, severely lacking in moisture content. It is likely that observations at these locations are capturing the steep moisture gradient at the airmass boundary, unable to be represented in ERA5 either due to i) ERA5's resolution or ii) the quality controls built in the assimilation scheme potentially filtering the profiles out triggered by large deviations between the observations and the forecasted values (Hersbach et al., 2020).~~**"**

"Observations from these research flights were not submitted to the Global Telecommunication System (GTS) for assimilation (Ehrlich et al., 2025) which explains why the observed steep moisture gradient at the airmass boundary is not represented in ERA5."

We also correct the following sentence in Sect. 2:

L105 - 106 : "The initialization of the trajectories at this location ~~serves a dual purpose: i) the use of more realistic ERA5 wind fields in this region at the time of initialization due to the abundance of dropsonde profiles available for assimilation (Hersbach et al., 2020), and ii)~~ **guarantees** more matches between trajectory and observational points which enables the comparison.**"**

- L214–219: This paragraph is describing the cloud radiative effect – is it possible to directly calculate the cloud radiative effect and plot it on the maps?

A: We calculated cloud radiative forcing (CRF) for shortwave and longwave radiation CRF_{SW} = SW_{sfc}^{cld} - SW_{sfc}^{clr} and CRF_{LW} = LW_{sfc}^{cld} – LW_{sfc}^{clr} using ERA5 data (Fig. AR1.3). The intruding airmass consistently contributes around 80 W m^{-2} uniformly across the transport corridor, wherever liquid clouds are present. We add this information in the discussion and offer the figure as supplementary material.

L244-252: " ~~The spatial distribution of the cloud water within the airmass is also reflected in the net shortwave radiation flux at the surface (Fig. 3d) during daytime. On the western flank of the airmass, where the LWP is larger, less solar radiation reaches the surface but the down-welling long-wave radiation emitted by the liquid clouds changes the sign ofthe net surface long-wave flux to positive (Fig. 3e).~~ **The net shortwave radiation along the path of the airmass is presented in Fig. 3d. At the time of the event (March 12-14), the Arctic receives roughly 7 to 11.4 hours of daylight depending on the latitude of interest. Therefore, solar radiation is only relevant for small parts of the airmass transformation. The surface shortwave radiative flux is largest near the south end of the trajectories (200 W m−2). Its spatial distribution mimics that of the liquid cloud water within the airmass (Fig. 3b). On the western flank of the airmass, where the LWP is larger, the liquid cloud blocks approximately up to 300 W m−2 of solar radiation (Fig. A1). In contrast, the liquid cloud consistently casts a longwave radiative forcing of around 80 W m−2 (Fig. A1) which changes the sign of the net surface long-wave flux to positive (Fig. 3e).**

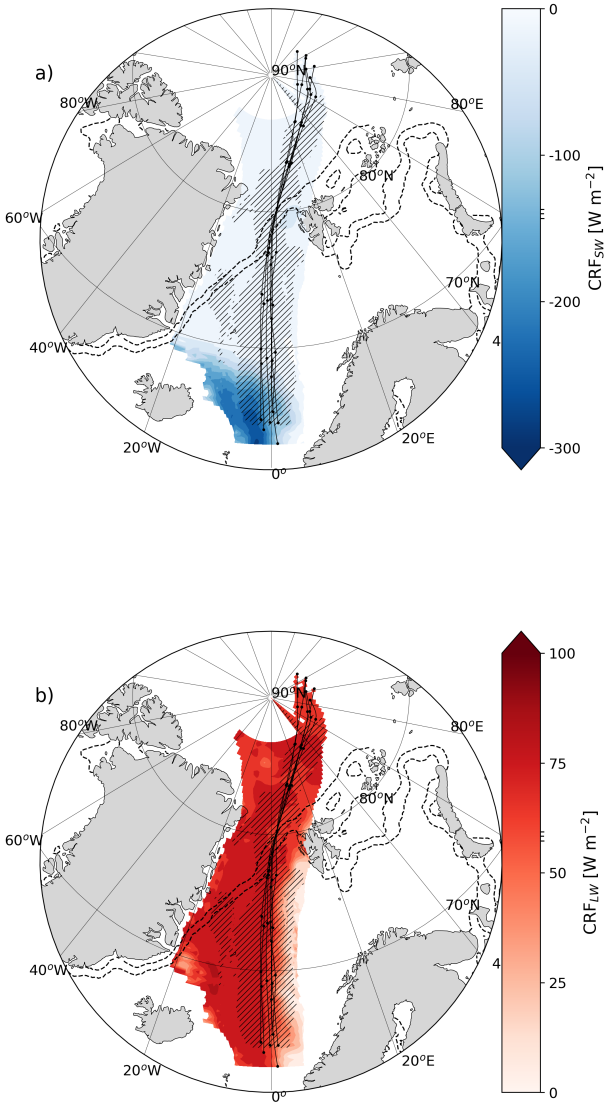

Figure AR1.3: Temporal evolution and spatial variability of the airmass during its poleward advection in terms of a) shortwave and b) long-wave radiative forcing. The trajectory ensemble is shown with black lines. Hatches mark the correlation range (see Sect. 2.3) around the airmass at

each timestep. Square markers, when present, correspond to the observed values. Dashed contours show boundaries of the MIZ, corresponding to sea-ice concentration values 0.15 and 0.8 on March 13, at 12 UTC.

- Fig. 4: I don't quite understand how cloud liquid and ice are represented in Fig. 4. Does the shaded area represent the additional atmospheric water in ice or liquid phase, in addition to the vapor-phase water (IWV)?

A: That is correct, the thickness of the shaded area represents the integrated cloud water content (liquid and ice) and the texture represents the phase (dots for liquid, no dots for ice). This information is now clearly stated in the figure caption.

"The width of the shaded areas attached to the right of the thick solid lines represents the vertically integrated total water path (TWP). Dots are used to show the portion that is in liquid phase (LWP)."

- Fig. 4: It is difficult to distinguish between the faded perpendicular lines for AOSCM/ERA5/IFS. Perhaps some could be plotted as dotted or dashed lines to make them easier to tell apart? Does each of these lines represent a timestep, such that the wider spacing of the lines over sea ice can be interpreted as faster air mass cooling and drying? Is appears that the uncertainty range is greater for the AOSCM than the other two products, is that correct?

A: We replotted the faded perpendicular lines in different styles to make them more distinguishable from each other (AR1.4). Spaces between these lines represent time intervals of 1 hour. The reviewer is correct to note that when the spacing becomes wider, the transformation accelerates. We now note this in the caption of Fig. 4:

"The faded lines are plotted with a time-step of 1 h, therefore their density signifies the speed of the transformation. "

The AOSCM uncertainty range is indeed larger than ERA5 and IFS-OF and it encompasses the curves of ERA5 and IFS-OF, as well as observations. The magnitude of the AOSCM ensemble uncertainty varies with time as a result of variability in the initial conditions and forcing. This is discussed in the manuscript in lines **L293-299**. Among other changes in this section, following the referees' suggestions, we have also added:

L297-298: "The increase in the AOSCM ensemble uncertainty is the combined result of the variability in the ensemble's initial conditions and alongstream forcing."

(*) Please note that we have recalculated the temperature averages shown in Fig. AR1.4 (Fig. 4 in the manuscript). In the previous version, the vertical averaging unintentionally gave greater weight to lower atmospheric levels due to the irregular vertical grid, resulting in higher values. The revised $\overline{T_{5km}}$ now properly accounts for vertical resolution.

While the updated temperature values appear generally lower, the structure of the curves remains largely unchanged. Therefore, the main characteristics of the airmass transformation remain clearly

visible: slope flattening over the MIZ, similarities in the heat-to-moisture trends across datasets, variations in uncertainty, and close agreement in the final airmass state. Related numerical values and minor visual differences resulting from the new calculation are properly reflected in the revised text (Sect. 3). These adjustments are minor and do not affect our main conclusions.

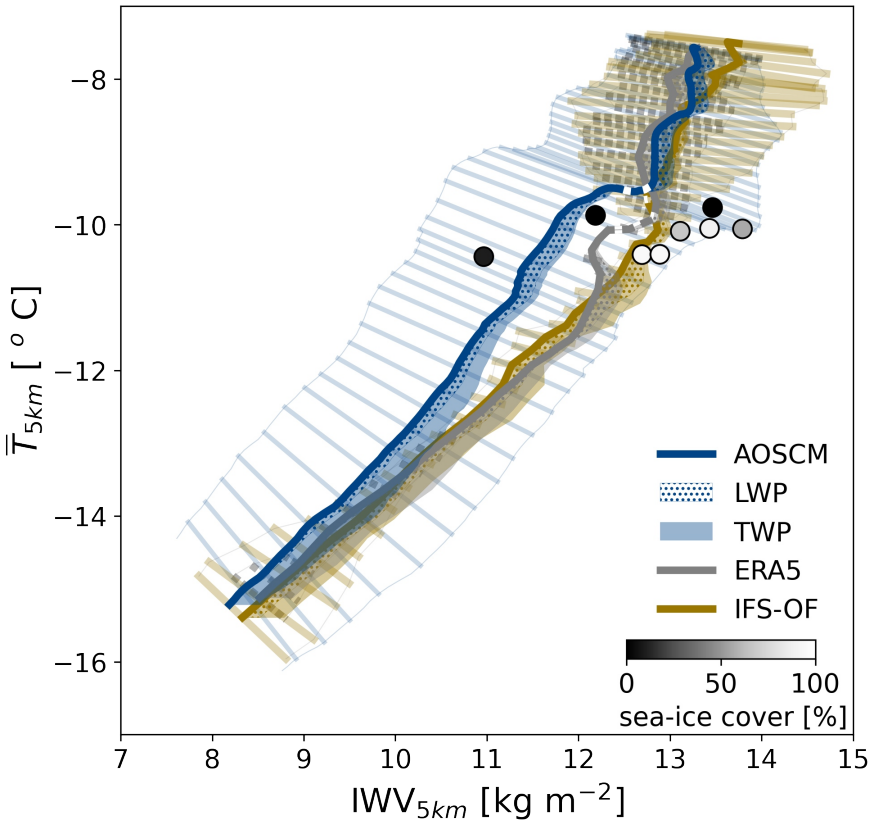

Figure AR1.4: Same as Fig. 4 in the manuscript with more distinguishable uncertainty range lines.

- L326–327: How was Bulk Richardson number = 0.25 chosen as the threshold for the boundary layer? Is this threshold based on previous studies?

A: This Bulk Richardson number threshold is used to diagnose the height of the boundary layer in ECMWF's Integrated Forecast System (IFS). IFS is the atmospheric component of AOSCM and the model used for the production of ERA5 and IFS-OF. Therefore, this diagnostic gives the most fair comparison of the boundary layer in all of the above products.

- Fig. 5: Is this figure created by averaging all the trajectories? Also, the uncertainty contours are difficult to see on the figure panels – perhaps they could be plotted with a darker color and/or thicker line.

A: Yes, the cross-sections presented in Fig. 5 are a product of averaging among the cross-sections of the individual trajectories. We made the uncertainty contours thicker so they can be more easily distinguished.

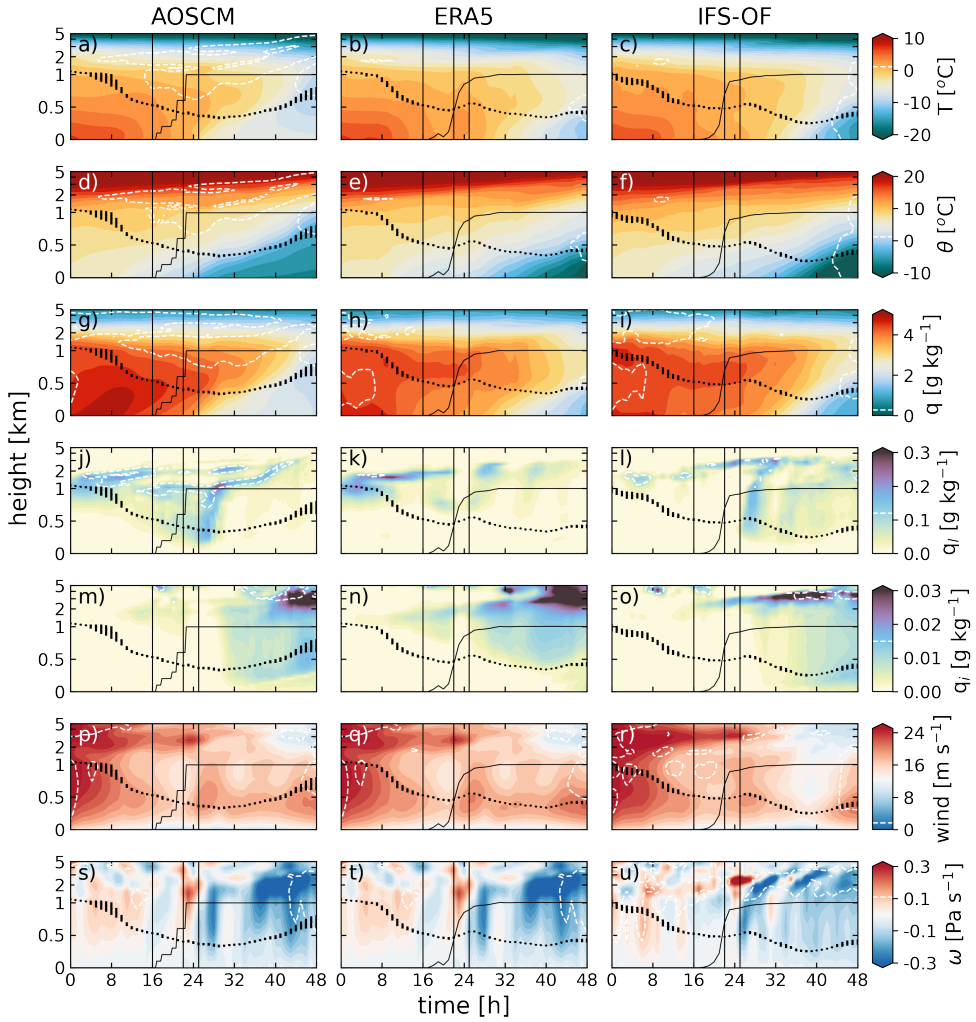

Figure AR1.5: Same as Fig. 5 in the manuscript but with thicker contours for ensemble uncertainty.

- L366–368: So are the ERA5 and IFS-OF representation of the boundary considered more reliable than the AOSCM?

A: Not necessarily. Sea-ice representation varies among the models we are considering in this study. The AOSCM resolves both sea-ice and snow properties and, in that sense, provides a more realistic boundary than ERA5 and IFS-OF in which sea-ice thickness is fixed to 1.5 m and the presence of snow is not taken into account. However, in our Lagrangian application, we divide the trajectories into smaller legs according to the sea-ice conditions and run consecutive simulations. In general, this helps the AOSCM reproduce important features of the airmass transformation, such changes in heat, moisture and cloud content and overall thermodynamic structure, but may affect the timing of others, especially close to the surface, such as the boundary layer evolution.

- L372: I think the reference to Fig. 5h is actually referring to Fig. 5k,h here? Please also check the other figure references in this paragraph (e.g. reference to Fig. 5i on L374).

A: The references are now pointing to the correct plots.

- L376: To my eye, it looks like the IFS-OF mostly shows a single-layer cloud structure for about 75% of the MIZ and early sea-ice leg.

A: It is true that the appearance of the low-level cloud is somewhat delayed in IFS-OF. The extent of the MIZ is smaller in IFS-OF which could be responsible for the delayed appearance of the low-level cloud. The multi-layer cloud structure is more prominent a few hours later and appears to be linked to the near-surface turbulent cooling the airmass experiences when advected over sea-ice.

- Fig. 6: I don't see several features on this figure that are described in the text. For example, where does AOSCM simulate a drop in temperature below freezing levels (L394–395)? L395 states that dropsondes released over full sea-ice cover show minor surface cooling, but it looks the dropsonde observations are within the envelope of the other temperature profiles in panel (k)?

A: Thank you for pointing this out. The drop below freezing levels does not occur for the AOSCM profile until over the "ice" leg. We rewrite this section to present the results more clearly:

L416-422: "Over the MIZ, the observed air temperature near the surface is slightly positive, approaching zero, which is consistent with the AOSCM, as well as ERA5 and IFS-OF (Fig. 6f). Dropsondes released over full sea-ice cover**, demonstrate a smaller surface cooling compared to the AOSCM ensemble mean (Fig. 6k). In the AOSCM, the near-surface temperature and specific humidity drop by approximately 4 °C and 1 g kg^{-1} respectively (Fig. 6k,l), as a response to the enforced decrease in skin temperature (see Table 1 and Fig. B1). ERA5 and especially IFS-OF match the observed thermodynamic structure near the surface while all products (including the AOSCM) are in agreement with observations over 500 m.** ~~The AOSCM seems to be more responsive to the advection over the sea-ice, showing a more dramatic reduction of temperature near the surface compared to the observations, ERA5 and IFS-OF (Fig. 6k,l)~~**"**

Note that the profiles Fig. 6 have been updated according to our new simulations in which the MIZ is now defined as the region with $0.15 \leq$ sea-ice concentration < 0.8, motivated by comments made by Referee #2.

- Fig. 6: Unless I am missing something, I don't see where the cloud liquid comparisons (right column) are addressed in the text.

A: We have now included a more elaborate discussion on the cloud liquid water profiles. In addition, we have rearranged the order of the subplots in Fig. AR1.6 (Fig. 6 in the manuscript) to enhance the flow of the discussion.

L428-436: "The airmass stratification remains strong over all surface types as demonstrated by the virtual potential temperature profiles, θ_v (Fig. 6c,~~f,g~~h,m). ~~Observations over ocean and, more so, the MIZ show small inversions within the first 2 km (Fig. 6f,g).~~ **Near the surface, agreement with the AOSCM is strong, except for over ice, where the simulated inversion appears much deeper,**

possibly due to the quick adjustment of the column to the more compact, colder sea-ice surface.

The AOSCM specific liquid cloud content shows an increase near the surface as the airmass is advected from the ocean (Fig. 6d) to the MIZ (Fig. 6i), indicating the formation of a secondary cloud layer that becomes even more prominent over fuller sea-ice (Fig. 6n). Cloud profile measurements were not conducted during these research flights. However, the observed thermodynamic profiles over ocean and, more so, the MIZ **and sea ice** show small inversions within the first 2 km (Fig. 6h,m). These inversions possibly correspond to a multi-layer cloud structure that agrees with our AOSCM simulations, as well as ERA5 and IFS-OF (Fig. 6~~j~~i-n).**"**

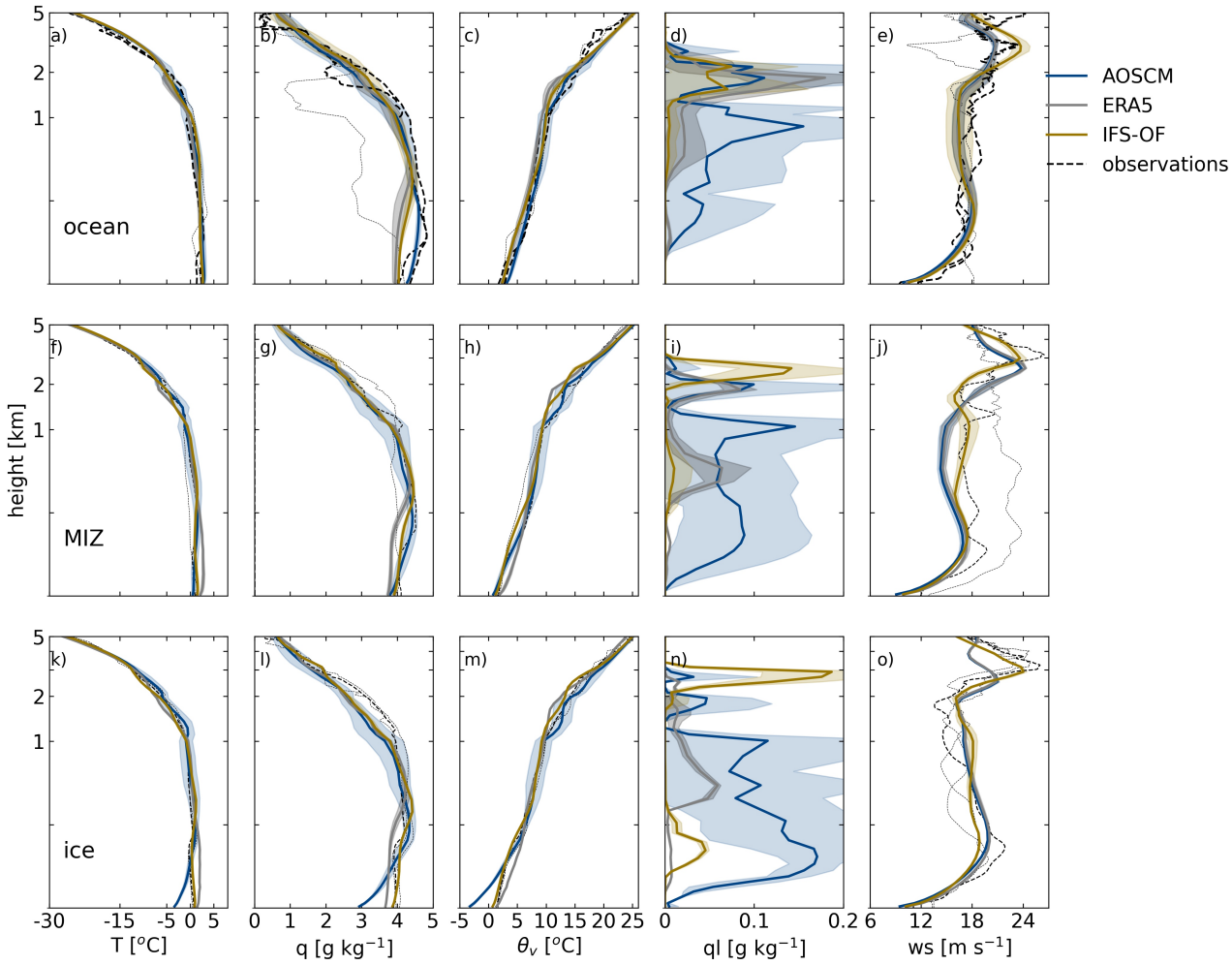

Figure AR1.6: Vertical profiles of temperature (°C), specific humidity (g kg^{-1}), potential temperature, **specific cloud liquid water content (g kg^{-1})** and wind speed **(m s^{-1})** ~~and specific cloud liquid water content (g kg−1)~~ over the ocean(a-e), MIZ(f-j) and sea ice(k-o). Observations are shown with black dashed lines; their thickness represents their proximity to the AOSCM (blue), ERA5 (gray) and IFS-OF (gold) reference profiles for each surface type. The reference profiles were taken

close to the majority of the observations (over or around the MIZ) and are denoted with black vertical lines in Fig. 5. The height axis is linear below 1 km and logarithmic above.

- L414–416: It sounds like it would be more accurate to call it the "liquid cloud layer" rather than the "cloud layer".

A: We added “liquid” in all instances where the cloud layer is referenced.

- Fig. 7: The caption does not describe panels e–g. Please check that all figure captions describe the figures in sufficient detail.

A: Panels e-g are now properly described in the caption.

We are also grateful for Referee #1’s technical corrections and for considerable amount of effort and attention to detail they dedicated to reviewing this manuscript. We have applied all of the edits listed below in the new version of the manuscript.

Technical corrections

- L3: "is" --> "are"

- L9: I think "simulate" or "reproduce" would be a better word choice than "emulate" here
- L26: Remove comma after "As"

- L42: "Airborn" --> "Airborne"

- L58: "imporant" --> "important"

- L68: "on" --> "to"

- L134: Add the word "are" after "tracks"

- L197: "dropping" --> "decreasing"

- L211: "air mass" --> "airmass" (to be consistent with the use of this word throughout the manuscript, I would argue that "air mass" is more commonly used in the literature but will leave it up to the authors whether they wish to change it throughout the manuscript)

- L216: Space needed in "of the"

- L293: "big" --> "large"

- L303: "uncertainty range ERA5 and IFS-OF curves" --> "uncertainty range of the ERA5 and IFS-OF curves" (?)

- L305: "and" --> "an"

- L307: "heat-to-moisture" --> "heat-to-moisture ratio" (?)

- L345: "while" --> "with" (?)

- L369: "dropping" --> "decreasing"

- L374: "bares" --> "bears"

- L391: "profiles" --> "profiles are" (?)

References

1. Ehrlich, A., Crewell, S., Herber, A., Klingebiel, M., Lüpkes, C., Mech, M., Becker, S., Borrmann, S., Bozem, H., Buschmann, M., Clemen, H.-C., De La Torre Castro, E., Dorff, H., Dupuy, R., Eppers, O., Ewald, F., George, G., Giez, A., Grawe, S., Gourbeyre, C., Hartmann, J., Jäkel, E., Joppe, P., Jourdan, O., Jurányi, Z., Kirbus, B., Lucke, J., Luebke, A. E., Maahn, M., Maherndl, N., Mallaun, C., Mayer, J., Mertes, S., Mioche, G., Moser, M., Müller, H., Pörtge, V., Risse, N., Roberts, G., Rosenburg, S., Röttenbacher, J., Schäfer, M., Schaefer, J., Schäfler, A., Schirmacher, I., Schneider, J., Schnitt, S., Stratmann, F., Tatzelt, C., Voigt, C., Walbröl, A., Weber, A., Wetzel, B., Wirth, M., and Wendisch, M.: A comprehensive in situ and remote sensing data set collected during the HALO–(AC)3 aircraft campaign, Earth System Science Data, 17, 1295–1328, https://doi.org/10.5194/essd-17-1295-2025, publisher: Copernicus GmbH, 2025.

2. Rinke, A., Cassano, J. J., Cassano, E. N., Jaiser, R., and Handorf, D.: Meteorological conditions during the MOSAiC expedition: Normal or anomalous?, Elementa: Science of the Anthropocene, 9, 00 023, https://doi.org/10.1525/elementa.2021.00023, 2021.685

3. Woods, C. and Caballero, R.: The Role of Moist Intrusions in Winter Arctic Warming and Sea Ice Decline, Journal of Climate, 29, 4473–4485, https://doi.org/10.1175/JCLI-D-15-0773.1, publisher: American Meteorological Society Section: Journal of Climate, 2016.